Available online at www.sciencedirect.com
ScienceDirect
Ceramics International 36 (2010) 2307–2314
CERAMICS INTERNATIONAL
www.elsevier.com/locate/ceramint

Crystallization behaviour and properties of multicomponent strontium—Containing lithia calcia silicate glasses

S.M. Salman *, S.N. Salama, H.A. Abo-Mosallam

Glass Research Dept., National Research Centre, El-Behoos St. Dokki, Cairo, Egypt

Received 17 February 2010; received in revised form 13 April 2010; accepted 4 June 2010
Available online 3 August 2010

Abstract

The crystallization behaviour of lithia calcia silicate system containing MgO, SrO, and Al_2O_3 has been investigated using DTA, XRD and SEM. The coefficient of thermal expansion and Vicker's microhardness of the obtained products were also evaluated. The main crystalline phases formed after different heat-treatments were lithium metasilicate, wollastonite, diopside, β-spodumene ss, pseudo-wollastonite, Sr_2SiO_4, $Sr_2Mg(Si_2O_7)$ and μ-$(Ca,Sr)SiO_3$. The wollastonite structure can accept considerable amount of strontium to form wollastonite strontium solid solution, while there is no solid solution of strontium in pseudo-wollastonite.

The dilatometric thermal expansion of the glass–ceramics was determined and exhibited a wide range of α-values depending upon the type and relative proportions of the crystalline phases formed. The α-values of the studied glass–ceramic ranged between 47 and 105 $\times 10^{-7}$ K^{-1} in the 25–600 °C temperature range. The microhardness values of the crystallized samples were 539–730 kg/mm^2. The compositions containing Al_2O_3 exhibited low thermal expansion and high microhardness values. The data obtained depend on the nature, concentration of crystalline phases formed and microstructure.

Keywords: D. Glass–ceramics; Crystallization; Expansion coefficients; Microhardness

1. Introduction

Glass–ceramics are polycrystalline solids produced by controlled crystallization of glasses [1]. Glass–ceramic properties depend on microstructure and composition of phases developed during the manufacturing process. The ability to control these two parameters depends on the original composition as well as the heat-treatment regime. Properties such as the coefficient of thermal expansion depend on the nature and volume of the phases developed, together with the thermal history [2].

The Li_2O–SiO_2 system is one of the best and most thoroughly studied glass–ceramic system involving controlled crystallization of glasses [3]. Barker et al. [4] studied the crystallization of lithia–silica glasses. The obtained results indicated that in the approximate range of 31–36 mol% Li_2O, a lithium disilicate solid solution is the primary nucleating phase, while for glasses containing more than approximately 36 mol% Li_2O, lithium metasilicate becomes the primary nucleating phase.

Shelby and Shelby [5] revealed that Li_2O–CaO–SiO_2 system is of interest because most of the glass-forming region lies within the immiscibility region. Salman et al. [6] studied the structure and crystallization process of a glass based on Li_2O–CaO–SiO_2 system. They found that the obtained glasses had high crystallization tendency upon heat-treatment and the crystallization was preceded without great difficulty through the entire volume over 700 °C. This is attributed to the phase separation of the lithia–silica glass that is caused by the incompatibility of Li_2O with SiO_2.

Lithium aluminosilicates, Li_2O–Al_2O_3–SiO_2, are interesting glass–ceramic systems that have attracted the attention from the technological point of view due to the glass–ceramics based on the β-quartz or β-spodumene solid solutions in the Li–aluminosilicate system have exceptionally low thermal expansion coefficients, good chemical durability and high-thermomechanical resistance [7,8]. The crystallization characteristics and properties of the eutectic (954 ± 4 °C) modified by partial replacements of Li_2O by Al_2O_3 and CaO by MgO or

* Corresponding author.
E-mail address: s.moghazy@yahoo.com (S.M. Salman).

0272-8842/$36.00
doi:10.1016/j.ceramint.2010.07.024

ZnO were investigated by Salman et al. [9]. They reported that the crystallization tendency was greatly enhanced by Al_2O_3 and MgO replacements. Wurtha et al. [10] studied the crystal growth of a complex glass based on the lithia–aluminosilicate system. They reported that during annealing, the SiO_2-concentration of the crystals increased continuously, and the β-quartz solid solution was depleted in Li_2O, MgO and Al_2O_3.

Wollastonite ($CaSiO_3$) is a calcium metasilicate. It has theoretical composition of 48.3% CaO and 51.7% SiO_2. Generally, there are three normal modifications of calcium metasilicate, pseudo-wollastonite (β-$CaSiO_3$), the high-temperature form, is triclinic (pseudo-orthorhombic), parawollastonite and wollastonite are both referred to as the low temperature modification (α-$CaSiO_3$) [11]. It is possible to incorporate strontium Sr^{2+} into the glass structure on a substitution basis for Ca^{2+}, as their respective ionic radii are similar. Large scale replacement of the calcium in wollastonite by strontium has been investigated in two synthetic phases [12].

The purpose of this work is to study the crystallization characteristics of a series of glasses based on lithia calcia silicate glasses containing MgO, SrO, and Al_2O_3 with the object to provide fundamental knowledge for the type of crystalline phase and solid solution formed of the studied glass–ceramic materials and studying their thermal and mechanical properties.

2. Experimental

2.1. Batch composition and glass preparation

The glass batches were prepared from reagent grade powders of Li_2CO_3, $CaCO_3$, $MgCO_3$, $SrCO_3$, Al_2O_3 and quartz (SiO_2). The details of the glass oxide constituents are given in Table 1. Reagent grade powders forming the glass batches were melted in Pt–2% Rh crucible, covered with Pt foil to minimize the evaporation, in an electric furnace with SiC heating elements at 1350–1400 °C for 3 h. Melting was continued until clear homogeneous melt was obtained; this was achieved by swirling the melt several times at about 30-min intervals. The melt was cast into rods and as buttons, which were then properly annealed in a muffle furnace at 500–550 °C to minimize the strain.

2.2. Differential thermal analysis (DTA)

The thermal behaviour of the finely powdered glass samples was examined using a SETARAM Labsys ^{TM}TG-DSC16. The powdered samples were heated in Pt-holder against another Pt-holder containing Al_2O_3 powder as a standard material. A uniform heating rate of 10 °C/min was adopted up to the appropriate temperature of the glasses. The results obtained were used as a guide for determining the heat-treatment temperatures applied to induce crystallization.

Table 1
Chemical compositions of the investigated glasses.

Glass no.	Oxide constitutions (mol%)					
	Li_2O	CaO	MgO	SrO	Al_2O_3	SiO_2
G_1	12	32	–	–	–	56
G_2	12	16	16	–	–	56
G_3	6	32	–	–	6	56
G_4	12	16	–	16	–	56
G_5	12	8	8	16	–	56
G_6	6	16	–	16	6	56

2.3. Thermal treatment

The progress of crystallization in the glasses was followed using double stage heat-treatment regimes. The glasses were first heated according to the DTA results at the endothermic peak temperature for 5 h, which was followed by another thermal treatment at the exothermic peak temperature for 10 h.

2.4. Material investigation

Identification of the crystal phases precipitating due to the course of crystallization was conducted by X-ray diffraction (XRD) analysis of the powdered samples. The X-ray diffraction patterns were obtained by using Bruker-AXS D8 Advance, with Ni filtered Cu Kα radiation. The reference data for the interpretation of the X-ray diffraction patterns were obtained from ASTM X-ray diffraction card files. The crystallization characteristics and internal microstructures of fractured surfaces of the crystalline samples, coated with gold spray, were examined by using scanning electron microscopy (SEM). Representative electron micrographs were obtained by using Jeol, JXA-840 Electron Probe Microanalyzer.

2.5. Thermal expansion measurements

The coefficients of thermal expansion (α-values) of the investigated samples were measured on 1.5 cm long rods using Linseis L76/1250 automatic recording multiplier dilatometer with a heating rate of 5 °C/min. The linear thermal expansion coefficient was automatically calculated using the general equation:

$$(\alpha) = (\Delta L/L)(1/\Delta T)$$

where (ΔL) is the increase in length, (ΔT) is the temperature interval over which the sample is heated and (L) is the original length of the specimen.

2.6. Microhardness

The microhardness of the crystallized samples was measured by using Vicker's microhardness indenter (Model Zwick/ZHV1-m microhardness tester). The specimens were cut using a low speed diamond saw, dry ground and polished carefully to obtain smooth and flat parallel surfaces of glass–ceramic samples before indentation testing. At least six indentation readings were made and measured for each sample. Testing was made using a load of 100 g; loading time was fixed for all the crystalline samples (15 s). The measurements were carried out under normal atmospheric conditions.

3. Results

3.1. Crystallization characteristics

The DTA data of the glasses (Fig. 1) showed endothermic effects in the 486–579 °C temperature range. These endothermic effects are attributed to the glass transition, at which the atoms begin to arrange themselves in preliminary structural elements subsequent to crystallization. Various exothermic effects in the 617–803 °C temperature range, indicating crystallization reaction in the glasses, are also recorded. The DTA data (Fig. 1) revealed that, the addition of (MgO/CaO), (Al_2O_3/Li_2O), (SrO + MgO)/CaO and (SrO + Al_2O_3)/(CaO + Li_2O) replacements led to shift the endothermic dips to higher temperatures, i.e., higher temperature is needed to start the nucleation process in the glasses. While, the addition of SrO instead of CaO led to shift the endothermic peak of the base glass G_1 to lower temperature.

The X-ray diffraction analysis (Table 2, Fig. 2, Pattern I) revealed that lithium metasilicate [Li_2SiO_3] (lines 4.69, 3.29, 2.70, Card No. 29-829) and wollastonite [$CaSiO_3$] (lines 3.51, 3.31, 3.08, 2.98, Card No. 29-372) were formed in the crystalline base glass G_1. However, on the addition of MgO instead of CaO (i.e., G_2, Fig. 2, Pattern II), diopside phase [$CaMgSi_2O_6$] (lines 3.23, 2.99, 2.95, 2.89, 2.52, Card No. 19-239) was developed instead of wollastonite phase together with the lithium metasilicate.

The addition of 6 mol% Al_2O_3 at the expense of Li_2O in crystalline glass G_3 led to the formation of lithium metasilicate

Table 2
Crystalline phases developed in the studied glass–ceramic samples.

Glass no.	Heat-treatment (°C/h)	Crystalline phases developed
G_1	505/5 h to 695/10 h	Li_2SiO_3 + Wollastonite
G_2	520/5 h to 730/10 h	Li_2SiO_3 + Diopside
G_3	575/5 h to 740/10 h	Li_2SiO_3 + Wollastonite + β-Spodumene ss
G_4	485/5 h to 745/10 h	Li_2SiO_3 + Sr_2SiO_4 + Pseudo-wollastonite
G_5	505/5 h to 740/10 h	Li_2SiO_3 + $Sr_2Mg(Si_2O_7)$ + μ-(Ca,Sr)SiO_3
G_6	580/5 h to 805/10 h	Li_2SiO_3 + μ-(Ca,Sr)SiO_3 + β-Spodumene ss

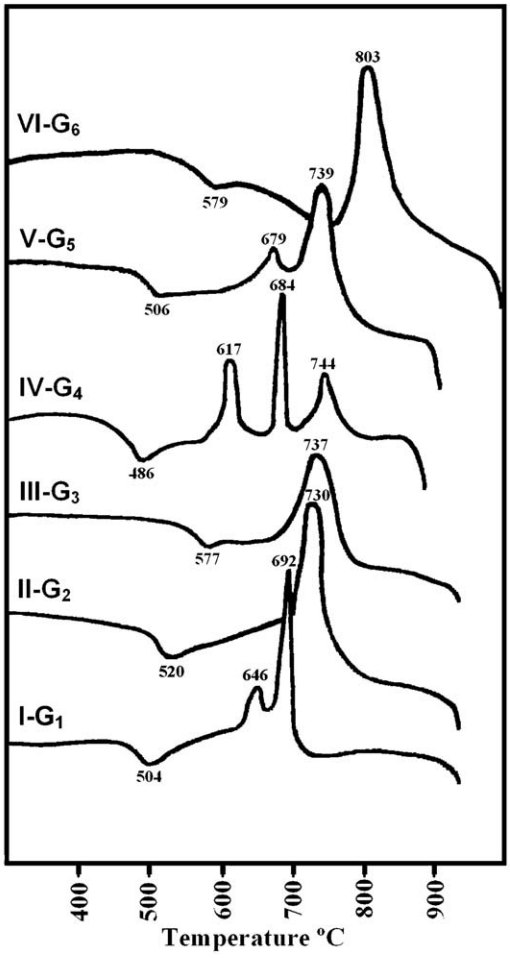

Fig. 1. DTA data of the investigated glass.

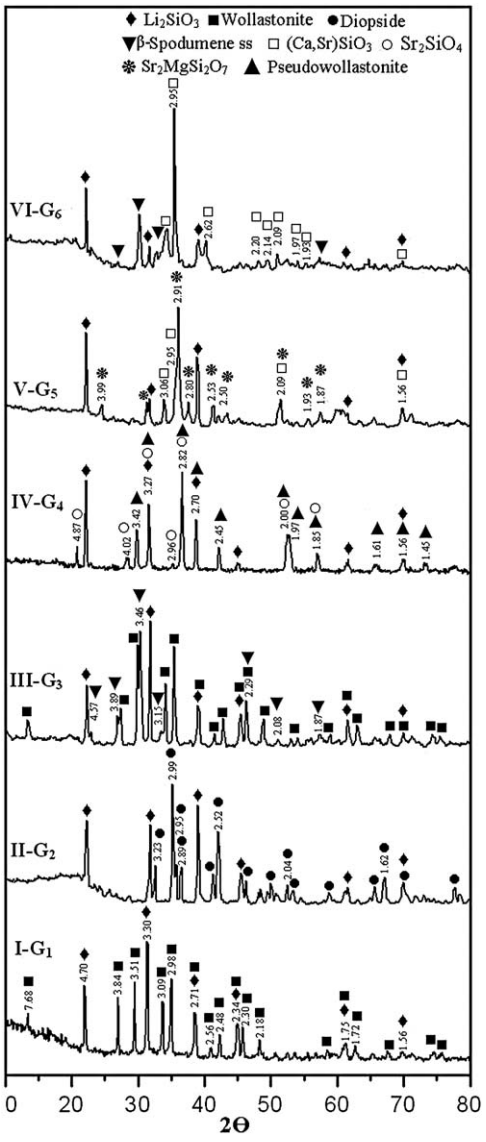

Fig. 2. XRD analysis of the crystallized glasses.

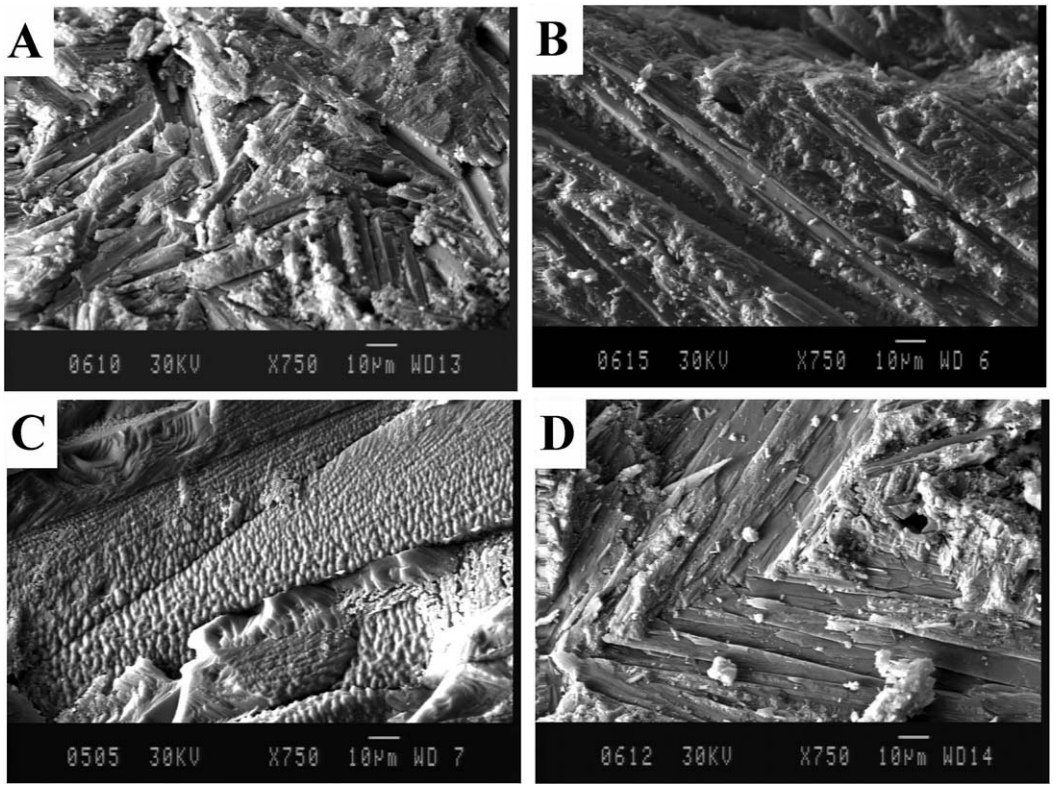

Fig. 3. Fracture surface micrographs of the crystallized glasses.

[Li_2SiO_3], wollastonite [$CaSiO_3$] and β-spodumene ss [$LiAlSi_3O_8$] (lines 4.58, 3.88, 3.47, 3.15, 1.88, Card No. 35-794) phases as indicated from XRD analysis (Fig. 2, Pattern III). The addition of SrO at the expense of CaO in glass–ceramic (i.e., G_4) led to the formation of lithium metasilicate, strontium silicate [Sr_2SiO_4] (lines 3.27, 2.80, 2.29, 2.12, 1.82, Card No.18-1281) and pseudo-wollastonite (lines 3.42, 3.24, 2.22, 2.82, 2.00, 1.97, Card No.31-300).

The XRD analysis (Fig. 3, Pattern V) of G_5 (with (MgO + SrO)/CaO replacements), revealed that lithium metasilicate, strontium magnesium silicate [$Sr_2Mg(Si_2O_7)$] (lines 3.89, 3.15, 2.94, 2.52, 2.09, 1.93, Card No. 75-1736) and calcium strontium silicate [μ-$(Ca,Sr)SiO_3$] (lines 2.99, 2.52, 2.09, 1.63, Card No. 15-314) were developed (Table 2). However, on the (Al_2O_3 + SrO)/(Li_2O + CaO) replacements (i.e., G_6, Fig. 2, Pattern VI), lithium metasilicate, calcium strontium silicate [μ-$(Ca,Sr)SiO_3$] and β-spodumene solid solution were formed.

The crystalline microstructure varied with composition as illustrated in Fig. 3. Scanning electron micrograph (SEM) of the fractured surface, (Fig. 3A), of the crystalline G_1, showed volume crystallization of blades-like structure. However, the effect of substitution of MgO instead of CaO (e.g. G_2) led to the formation of fine fibrous microstructure (Fig. 3B). In the G_3 (with Al_2O_3/Li_2O replacement), volume crystallization of tiny aggregates were formed (Fig. 3C). However, prismatic-like growths were developed in case of glass G_4 (with SrO/CaO replacement), Fig. 3D.

3.2. Thermal expansion

The coefficients of thermal expansion (CTE) of the investigated glass–ceramics obtained after heat-treatment are given in (Table 3 and Fig. 4). The CTE values range from 47 to $105 \times 10^{-7}\ K^{-1}$. The composition dependence of the expansion coefficient relationship (Fig. 4) showed that the replacements in

Table 3
Thermal expansion and Vickers hardness values of the investigated glass–ceramic.

Sample no.	Thermal expansion coefficients-α + $10^{-7}\ K^{-1}$					Hv (kg/mm^2)
	25–200	25–300	25–400	25–500	25–600	
G_1	91	93	94	97	101	600
G_2	80	83	85	86	87	648
G_3	47	49	50	52	53	710
G_4	93	94	97	100	98	539
G_5	97	99	101	103	105	682
G_6	59	61	62	64	67	730

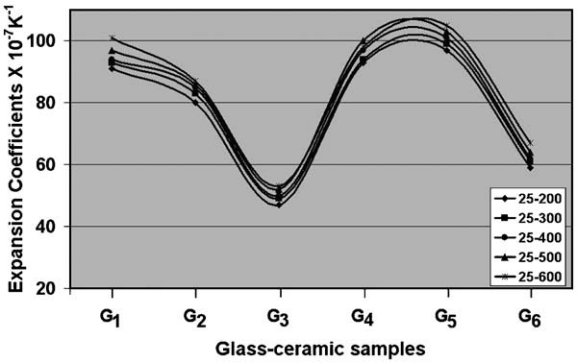

Fig. 4. The thermal expansion coefficient of glass–ceramic sample at different temperature.

the base glass of MgO by CaO i.e., G_2, Al_2O_3/Li_2O i.e., G_3 and $(SrO + Al_2O_3)/(CaO + Li_2O)$ i.e., G_6 generally decreased the α-values of the crystalline materials. However, the addition of SrO at the expense of CaO and (MgO + SrO)/CaO replacement increase the expansion coefficient values of the glass–ceramics (i.e., G_4 and G_5, respectively Table 3, Fig. 4).

3.3. Microhardness

The Vicker's microhardness values were determined for the resulting glass–ceramics. The obtained data are exhibited in Table 3. The data are also represented in Figs. 5 and 6. The glass–ceramic samples have Vickers' hardness values in 539–730 kg/mm^2 range. The value of sample G_4 (with SrO/CaO replacement) exhibits the lowest hardness value, while the sample G_6 (with $(SrO + Al_2O_3)/(CaO + Li_2O)$ replacement) represents the highest value.

4. Discussion

4.1. Crystallization characteristics

The progress of crystallization in the glasses, the type and proportions of the crystalline phases formed were markedly dependent on the variation of the glass oxide constituents and the extent of oxides replacements. The addition of MgO instead of CaO in the glass sample G_1 and in SrO-containing glasses increases the temperature at which the nucleation begins. The

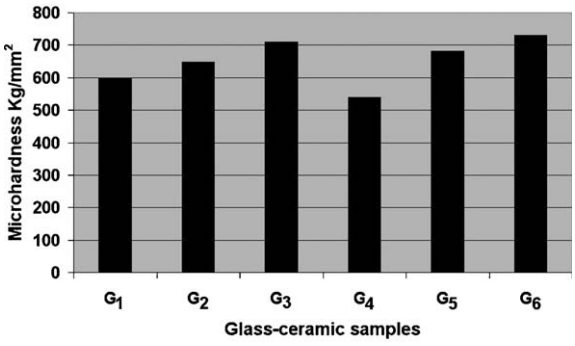

Fig. 5. Microhardness value of the crystallized samples.

DTA data revealed that the endothermic dip peak was shifted to higher temperatures by MgO/CaO in the studied glass. This could be attributed to role played by MgO in the glass structure, the field strength of Mg^{2+} (4.73) is higher than that of Ca^{2+} (2.04) [13]. It is expected, therefore, that the addition of MgO at the expense of CaO led to increase of the coherency of glass structure and to increase the nucleation temperature of these glasses.

The addition of Al_2O_3 at the expense of Li_2O in the base glass G_1 and in SrO-containing glass led to shift the dips of the endothermic peaks towards higher temperatures. This could be rationalized on the basis that the ability of aluminum as an intermediate oxide to form the AlO_4 group or to be housed in octahedral coordination in the glass interstices [14]. The present results indicate that Al^{3+} preferably exhibited a tetrahedral coordination in the glass and this led to increase the connectivity of the glass structure, which could explain the shift of endothermic peaks towards higher temperature values.

On the other hand, the glass transition temperature (T_g) decreased with substitution of strontium for calcium in the glasses. This could be attributed to the fact that a disruption in the glass network may occurred by the slightly larger strontium cation due to the weaker strontium–oxygen bond strength [15].

The crystallization of the base glass G_1 had high crystallization tendency upon heat-treatment and the crystallization occurred without great difficulty. This may be explained by the phase separation of the lithia–silica glass that is caused by the incompatibility of Li_2O with SiO_2 [5]. The X-ray diffraction analysis indicated that base glass G_1 crystallized into wollastonite and lithium metasilicate phases. Wollastonite–$CaSiO_3$ is one of the most important mineral phases of the pyroxenoid group. The pyroxenoid minerals are inosilicates of the general formula $XSiO_3$. The X, represents ions such as calcium, sodium, magnesium, iron and manganese [11]. Mishima et al. [16] reported that the lithium metasilicate crystals grew linearly with heating time and the rate of crystal growth increased with temperature. The MgO/CaO replacement in the base glasses (i.e., G_2) favour the formation of lithium metasilicate together with a diopside phases. The crystalline material containing-diopside ($CaMgSi_2O_6$) showed good mechanical properties and excellent thermal properties [17].

It is well known that compositions crystallizing to give solid solution series are important to control the properties of the resultant materials and offer an excellent opportunity to the glass–ceramic study. The addition of Al_2O_3 at the expense of Li_2O in the base glass (i.e., G_3) led to form lithium metasilicate, wollastonite and β-spodumene ss ($LiAlSi_3O_8$) as indicated from the shift of d-spacing lines of (XRD) characteristics for the $LiAlSi_2O_6$ phase towards higher 2θ values. It seemed, therefore, that there is a preferential tendency for β-spodumene ($LiAlSi_2O_6$) to capture $nSiO_2$ in its structure. Guo et al. [18] reported that there is a transformation of hexagonal $LiAlSi_2O_6$ into tetragonal lithium orthoclase $LiAlSi_3O_8$ which is a solid solution of β-spodumene and SiO_2. This proves that spodumene mineral changes the formation and transformation of main crystallization by adding other oxides (such as SiO_2) into the $LiAlSi_2O_6$ to form a new solid solution. In the crystallization of lithium calcium silicate glassy system Al_2O_3

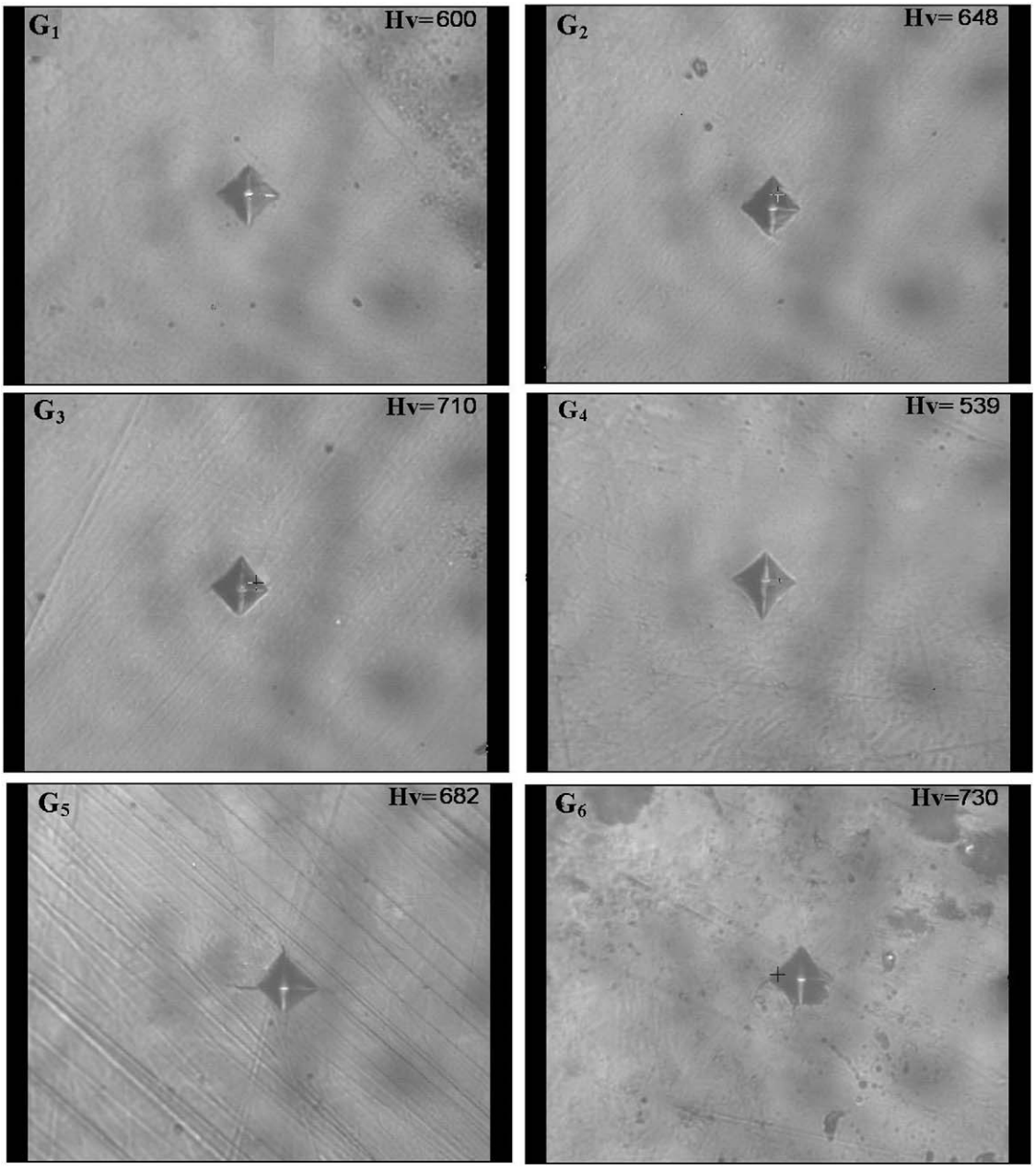

Fig. 6. The Vickers micro-indent of glass–ceramic samples.

should be first combined with an equivalent amount of Li_2O and SiO_2 to form lithium–aluminosilicate. If there is an excess of Li_2O over Al_2O_3 in molar ratios, it can then combine with silica or calcium to form lithium silicate or lithium calcium silicate phases [9]. The formation of lithium metasilicate [Li_2SiO_3] may be attributed to the fact that the tendency of β-spodumene to form a solid solution with silica rendering the residual glass are poor in silica therefore metasilicate could be formed [19].

The addition of SrO at the expense of CaO in G_4 led to the development of lithium metasilicate, strontium silicate [Sr_2SiO_4] and pseudo-wollastonite phases. There is no preferential tendency for pseudo-wollastonite to accommodate strontium in its structure therefore, strontium silicate phase could be formed. Wollastonite can capture up to 21% of diopside in its structure. However, there is no solid solution of diopside in pseudo-wollastonite [11]. Salman [20] found that the transformation of pseudo-wollastonite to wollastonite is very sluggish. However, he concluded that, pseudo-wollastonite could be formed as an intermediate stage during the crystallization of wollastonite below the inversion temperature of wollastonite ↔ pseudo-wollastonite transformation.

Mineralogically, the (MgO + SrO)/CaO replacement in the base glass, i.e., G_5, led to the formation of lithium metasilicate, strontium magnesium silicate [$Sr_2Mg(Si_2O_7)$] and calcium strontium silicate [μ-(Ca,Sr)SiO_3]. The X-ray diffraction analysis revealed that lithium metasilicate, calcium strontium silicate [μ-(Ca,Sr)SiO_3] and β-spodumene solid solution were formed due to (Al_2O_3 + SrO)/(Li_2O + CaO) replacements i.e.,

G_6. The formation of [μ-(Ca,Sr)SiO_3] instead of wollastonite [$CaSiO_3$] in the base glass may be attributed to preferential tendency for $CaSiO_3$ to capture SrO in its structure. A structure containing Si_3O_9 rings was originally proposed for high-temperature $CaSiO_3$, and the structurally analogous $SrSiO_3$ and $SrGeO_3$ [21]. Dornberger-Schiff [22] suggested that these structures form a series of polytypes, with some minor changes in the symmetry of the Si_3O_9 or Ge_3O_9 rings. Large scale replacement of the calcium in wollastonite ($CaSiO_3$) by strontium has been investigated in two synthetic phases $Ca_{3.12}Sr_{1.24}Si_4O_{12}$ and $Ca_{1.O2}Sr_{o.84}Si_2O_6$. The phases produced show both disordered stacking sequences and ordered polytypes, which can be related to previous polytypic modifications in ring silicates [12]. The incorporation of Sr into $CaSiO_3$ resulted decreased its ionic dissolution rate, improved physical and biological properties as compared with pure $CaSiO_3$ ceramics [23].

4.2. Thermal expansion

The change of CTE values of the investigated glass–ceramic samples is governed by the type and quantity of the developed crystalline phases, as well as, by the amount and composition of the residual glassy matrix. Extremely wide ranges of thermal expansion coefficients are covered by the different crystal types and the development of these phases in appropriate proportions forms the basis of the production of glass–ceramics with controlled thermal expansion coefficient [24]. The contribution of a particular crystal phase to the thermal expansion of a glass–ceramic may also be modified if the crystal enters into solid solution with another phase.

An extremely wide range of the thermal expansion coefficients is covered by the different crystal types and the development of these phases in appropriate proportions, forms the basis of the production of glass–ceramics with controlled thermal expansion coefficients. The expansion coefficient of β-spodumene and its solid solution have low positive value (3–9) $\times 10^{-7}\,K^{-1}$ 20–700 °C [25]. Wollastonite has α-value of $94 \times 10^{-7}\,K^{-1}$ 100–200 °C [26], diopside which is related to the pyroxene-type phases, has α-values of $78 \times 10^{-7}\,K^{-1}$ 24–1000 °C [27].

The present results revealed that the addition of MgO instead of CaO led to a decrease of the expansion coefficient of the resulting glass–ceramics. This may be attributed to the formation of relatively low-expanding diopside phase at the expense of the high-expanding orthorhombic wollastonite phase. On the other hand, the decrease in the α-values was also observed by (Al_2O_3/Li_2O) and ($SrO + Al_2O_3$)/($CaO + Li_2O$) replacements in base glass. This may be attributed to the formation of a low-expanding β-spodumen ss phase [25]. Progressive increases in the α-values were observed in G_4 and G_5 samples. This may be attributed to the formation of a very high-expanding strontium silicate phases.

4.3. Microhardness

The microhardness of material is often equated with its resistance to abrasion or wear and this characteristic is of practical interest since it may determine the resistivity of a material during use and it may also decide the suitability of the material for special applications. According to Miska [28] the microhardness of crystallized glasses depends not only on the type of precipitating phases but also on their size, shape, and natural wetting as well on the emergence or absence of internal cracks. However, the degree of crystallinity should be also taken into consideration.

The addition of MgO at the expense of CaO and (MgO + SrO)/CaO replacement in the base glass (G_1) increased the microhardness values of the investigated glass–ceramics (G_2 and G_5). This may be due the formation of fine microstructure as indicated from the SEM micrograph of the glass–ceramics of G_2 (Fig. 3B), as compared with that of microstructure formed in the glass–ceramic of G_1 (Fig. 3A). This also may be due to the formation of relatively higher hardness diopside phase instead of wollastonite phase in G_2. Park et al. [29] indicated that glass–ceramics containing large amount of diopside phase generally showed a high microhardness value due to the interlocking microstructures of diopside crystals with microhardness value 6730 MPa. The increase of microhardness value measured for the crystalline glasses, G_3 and G_6 may be due to the formation of highly hardness β-spodumene solid solution phase. Crystallization of β-spodumene improves the microhardness values; this due to the presence of spodumene significantly reduces the porosity and improves the densification [30]. The low microhardness value (539 kg/mm^2) measured for the crystalline glass, G_4, may be due to the formation of coarse microstructure as indicated from SEM (Fig. 3D) and also to the crystallization of low microhardness crystalline phases.

5. Conclusions

Glass compositions based on multicomponent strontium lithia calcia silicate glasses using suitable heat-treatment regime were investigated. A wide range of thermal properties and good mechanical behaviour glass–ceramic samples were obtained.

References

[1] G.H. Beall, L.R. Pinckney, Nanophase glass–ceramics, Journal of American Ceramic Society 82 (1999) 5–16.
[2] W. Höland, G. Beall, Glass–Ceramic Technology, The American Ceramic Society, Westerville, OH, USA, 2002, pp. 43081..
[3] W. Holland, E. Apel, Ch. Vant Hoen, V. Rheinberger, Studies of crystal phase formation in high strength lithium disilicate glass–ceramics, Journal of Non-Crystalline Solids 352 (2006) 4041–4050.
[4] M.F. Barker, T.H. Wang, P.F. James, Nucleation and growth kinetics of lithium disilicate and lithium metasilicate in lithia–silica glasses, Physics and Chemistry of Glasses 29 (1988) 240–248.
[5] J.E. Shelby, S.R. Shelby, Phase separation and the properties of lithium calcium silicate glasses, Physics and Chemistry of Glasses 41 (2000) 59–64.
[6] S.M. Salman, H. Darwish, E.A. Mahdy, Crystallization characteristics and physico-chemical properties of the glasses based on Li_2O–CaO–SiO_2 eutectic (954 °C) system containing magnesium oxide, Ceramics International 34 (2008) 1819–1828.
[7] B. Aitken, G.H. Beall, Material science and technology series, in: Cahn, et al. (Eds.), Glass–ceramics, vol. 11, 1994, pp. 269–294 (chapter 5).

[8] X. Guo, H. Yang, M. Cao, Nucleation and crystallization behaviour of Li_2O–Al_2O_3–SiO_2 system glass–ceramic containing little fluorine and nofluorine, Journal of Non-Crystalline Solids 351 (2005) 2133–2137.
[9] S.M. Salman, H. Darwish, E.A. Mahdy, The influence of Al_2O_3, MgO and ZnO on the crystallization characteristics and properties of lithium calcium silicate glasses and glass–ceramics, Material Chemistry and Physics 112 (2008) 945–953.
[10] R. Wurtha, F. Munoz, M. Müller, C. Rüssel, Crystal growth in a multicomponent lithia aluminosilicate glass, Material Chemistry and Physics 116 (2009) 433–437.
[11] W.A. Deer, R.A. Howie, Zussman, An introduction to the rock forming minerals Third ELBS impression, Common Wealth, Printing Press Ltd., Hong Kong, 1992.
[12] W.S. Lin, D.A. Jefferson, J.M. Thomas, Replacement of calcium by strontium in the wollastonite structure: an electron microscopy study, Material Research Bulletin 15 (1980) 1643–1648.
[13] R.H. Doremus, Glass Science, 2nd ed., John Wiley and Sons Inc., N. Y, 1994.
[14] J.H. Park, D.J. Min, Effect of fluorspar and alumina on the viscous flow of calcium silicate melts containing MgO, Journal of Non-Crystalline Solids 337 (2004) 150–156.
[15] R.G. Hill, A. Stamboulis, R.V. Law, A. Clifford, M.R. Towler, C. Crowley, The influence of strontium substitution in flouroapatite glasses and glass–ceramics, Journal of Non-Crystalline Solids 336 (2004) 223–229.
[16] N. Mishima, T. Wakasugi, R. Ota, Nucleation behaviour of Li_2O–Na_2O–SiO_2 doped with platinum J, Ceramic Society of Japan 112 (2004) 350–353.
[17] Y.J. Park, J. Heo, Conversion to glass–ceramics from glasses made by MSW incinerator fly ash for recycling, Ceramics International 28 (2002) 689–694.
[18] X. Guo, L. Zhang, I. Yang, Effects of Li replacement on the nucleation, crystallization and microstructure of Li_2O–Al_2O_3–SiO_2 glass, Journal of Non-Crystalline Solids 354 (2008) 4031–4036.
[19] S.N. Salama, S.M. Salman, H. Darwish, Contributions of alumina and magnesia to crystallization characteristics of some lithium borosilicate glasses, Silicates Industries 11–12 (1996) 263–271.
[20] S.M.Salman, Study of the crystallization process in melts and glassy products obtained from granitic and carbonate rock mixtures, M.Sc. Thesis, Cairo University, 1970.
[21] W. Hilmer, An X-ray investigation of strontium germanate $SrGeO_3$, Soviet Physics-Crystallography 7 (1963) 573–576.
[22] K. Dornberger-Schiff, The symmetry and structure of strontium germanate, $Sr(GeO_3)$, as a structural model for a-wollastonite, $Ca(SiO_3)$, Soviet Physics-Crystallography 6 (1962) 694–700.
[23] Ch. Wu, Y. Ramaswamy, D. Kwik, H. Zreiqat, The effect of strontium incorporation into $CaSiO_3$ ceramics on their physical and biological properties, Biomaterials 28 (2007) 3171–3181.
[24] W. McMillan, Glass Ceramics, Academic Press, London, NY, 1979.
[25] G. Muller, Structure, composition, stability and thermal expansion of high eucryptite and keatite type aluminosilicate, in: H. Bach (Ed.), Low Thermal Expansion Glass–Ceramic, 2nd ed., Springer-Verlag, Berlin, 1995, pp. 13–25.
[26] Z. Strnad, Glass–Ceramic Materials Glass Science and Technology, vol. 8, Elsevier, Amsterdam, 1986.
[27] L.W. Finger, A. Ohashi, C.W. Burnharn, Effect of calcium–iron substitution on the clinopyroxene crystal structure, American Mineralogist 61 (1974) 303.
[28] H.A. Miska, Ceramics and glasses, Engineered Materials Handbook, 4 ASM Int., vol. 4, 1991.
[29] Y.J. Park, S.O. Moon, J. Heo, Crystalline phase control of glass–ceramics obtained from sewage sludge fly ash, Ceramics International 29 (2003) 223–227.
[30] C.G. Shi, I.M. Low, Effect of spodumene additions on the sintering and densification of aluminum titanate, Material Research Bulletin 33 (1998) 817–824.